Electronic Supplementary Material (ESI) for Lab on a Chip
This journal is © The Royal Society of Chemistry 2024

Electronic Supplementary Information

DRUG TESTING OF MONODISPERSE ARRAYS OF LIVE MICRODISSECTED TUMORS USING A VALVED MULTIWELL MICROFLUIDIC PLATFORM

Ethan J. Lockhart[1], Lisa F. Horowitz[1], Adán Rodríguez[1], Songli Zhu[2], Tran Nguyen[1], Mehdi Mehrabi[3], Taranjit S. Gujral[2], and Albert Folch[1]

[1]Department of Bioengineering, University of Washington, Seattle, USA
[2]Human Biology Division, Fred Hutchinson Cancer Research Center, Seattle, USA
[3]L&T Technology Services, Meta Reality Labs

Supplementary Methods

CNC milling device components in PMMA

Computer-aided manufacturing of the microfluidic device

Computer-aided manufacturing (CAM) tools facilitated prototype development via CNC milling. 3D models imported into Fusion 360 enabled generation of milling toolpaths through simple selection of regions and specifying milling parameters. Once defined, simulated toolpaths revealed potential tool collisions (***e.g.***, cutting too deep with a particular endmill) and aided with prototype visualization. Since toolpath editing or simulation of the whole device often crashed the program, we reduced computational intensity by segmenting the large channel networks into 4 smaller sections using sketch outlines. Then, we selected these smaller sketch regions within separate milling operations to generate the toolpaths. Thus, segmentation of larger geometrical features using sketches reduced loading times for editing and simulation.

Surface profiling to account for PMMA thickness variability

Stock PMMA plastic sheets have significant thickness tolerances. Many plastic manufacturers use cell casting to create high-quality PMMA sheets wherein liquid monomer is deposited between two glass sheets before polymerizing. However, the glass sheets may sag during the process, creating irregular surface topography that has significant thickness variability ($\sim \pm 20\%$ of the stock thickness). Consequently, variable plastic thickness complicates spindle height calibration, leading to inconsistent cutting depths. This issue becomes particularly pronounced when milling across multiwell plate-sized surface areas as with our device (Fig. 2). For us, the plastic thickness fluctuated enough to inhibit endmill contact with the plastic when cutting shallow features complicating production of our valves (50 μm in depth - less than the thickness tolerance of the plastic, shown in Fig. 4a). To overcome this challenge for milling, we used the “surface profile” function of our mill (DATRON neo) which measures a maximum of 2,000 evenly spaced calibration points within a defined cutting area using a pressure-sensing calibration probe. Using these points, the machine extrapolates an irregular surface profile to calculate height compensation. The accuracy of the extrapolated surface profile increases with the number of points measured at the expense of time. Overall, surface profiling enhances plastic microfabrication, enabling milling of small features across large surface areas.

Cleaning CNC-milled components

Following CNC milling, a series of washing steps was necessary to remove burrs and plastic debris. For each layer except the TPU, we used a gloved hand to scrub and spread liquid dish soap on both sides. Then, we rinsed the layers with water and dried them with an air gun. A dry toothbrush or metal pick removed the remaining burrs. We angled the toothbrush head to ensure the bristles reached into channels and through-holes. Repeated soap, water, and pressurized air removed the remaining debris. We stored all layers in clean, covered containers.

Device assembly

Bonding PMMA layers

We began device assembly by using our previously reported thermal solvent bonding process to join the microchannel layer (MCL) and valve seat layer (VSL) together (Fig. 2a).[1] Briefly, PMMA becomes slightly adhesive when exposed to chloroform vapor, causing polymer reflow.[2,3] An irreversible cohesive bond forms when two exposed surfaces are pressed together, allowing assembly of PMMA layers. As an additional benefit, treatment with chloroform vapors also reduces surface roughness caused by mill marks, improving optical quality. To begin bonding, we placed the MCL on four steel standoffs (3 mm-elevation) resting inside a glass container (11-cup, Pyrex) filled with 50 mL of chloroform to expose the bottom (open channel side) for 2 min. Then, we transferred the layer from the container onto a PMMA alignment tool with the exposed side facing up before replenishing evaporated chloroform. The plastic alignment tool consisted of a PMMA block with holes at the corners to fit four metal pins (5 mm diam. x 15 mm length). The pins corresponded to through-holes in each layer of the device (see Fig. 2a), enabling registration and alignment. We continued the process by exposing the top (featureless side) of the VSL for 3 min before rapidly (within 15 sec) transferring the exposed face onto the MCL.

Manual compression joined the layers with a weak-bond. We removed the layers from the alignment tool, then sandwiched them between two 3 mm-thick polydimethylsiloxane (PDMS) slabs. To achieve permanent bonding, a heat press (Carver Model 4386, Carver Inc., USA) compressed the layers for 6 min at 140 ºF and 350 psi. We flipped and repositioned the stack before pressing for an additional 2 min at 140 ºF and 220 psi. Afterwards, we removed the PDMS slabs and clamped 10 medium paper binder clips around the perimeter of the bonded layers to prevent separation as the plastic cooled for 2 hrs.

Bonding TPU to PMMA layers

We continued assembly by joining the bonded MCL/VSL layers to the pneumatic control layer (PCL) via sandwiching a flexible polymer layer in between (Fig. 2a). This process[4,5] (referred to as "thermal fusion bonding") created the thermoplastic microvalves in our device using temperature, pressure, and time by bonding thermoplastic polyurethane (TPU, PT9200US NAT, Covestro LLC, USA) between two adjoining PMMA layers in a sandwich. Normally, thermoplastics trap gases and chemicals within their bulk polymer structure and release them upon heating. However, when stacking thermoplastic layers for the thermal fusion bonding process, exiting gas bubbles remain trapped between layers. For thermoplastic TPU microvalves, the bubbles can deform and irreversibly collapse the TPU film, blocking flow in microchannels; they also prevent contact between the TPU and PMMA layers and weaken bond strength. Therefore, exposing plastic layers to heat and negative pressure before stacking prevents bubble entrapment.

Bonding TPU to PMMA began with a series of washing and thermal treatment steps to remove entrapped gases and chemicals from the bulk of the thermoplastic materials. For all PMMA layers, we washed the surfaces with liquid dish soap and water then dried with pressurized air. Ethanol-soaked lint-free wipes (Pro-Wipe 750, Berkshire, USA) removed the remaining residue. Then, we placed the PMMA layers in a vacuum oven (Isotemp vacuum oven 280A, Fisher Scientific, USA) at 80 ºC and -12 psi (gauge pressure) for at least 8 hrs. We removed the layers from the oven and repeated washing with soap, water, and ethanol, then stored the layers in a clean container. Using a razor blade, we cut a piece of fresh TPU from a stock roll of film to have slightly larger outer dimensions than the device, then scrubbed the film with ethanol. A pressurized air blow gun removed excess ethanol from the TPU film. Next, we treated all PMMA and TPU layers in the vacuum oven together at 50 ºC and -12 psi for 100 min.

Next, we assembled the layers in several phases. First, we applied PDMS base elastomer (PDMS part B) to the valve seats as an "anti-bond" to prevent TPU adhesion. We dipped tweezers in PDMS part B, then dragged the tip across each seat. Spillover could prevent bonding in necessary regions, so we used laboratory swabs to clean off excess solution from regions outside the valve seats. Afterwards, we placed the TPU film flat over the whole surface of the valve seat layer. A laminator (Sky, 325R6) set at 110 ºC eliminated wrinkles in the TPU film and created a temporary bond that held the TPU in place for the rest of the assembly. We first set the laminator to speed 9 to assist initial insertion of the layers, then we switched to speed 3 to lengthen lamination time. Once laminated, a scalpel removed TPU from covering the pneumatic control inlet shared by the bonded MCL/VSL layers (see Fig. 2a,b, inlet hole on left side of device). Afterwards, we aligned the MCL/VSL to the pneumatic control layer. For the alignment process, we placed the MCL/VSL layer onto fresh tinfoil with the TPU facing up. We placed the PCL onto our alignment tool (see "*Bonding PMMA layers*") with the channel side facing up. Then, we flipped the alignment apparatus and inserted its pins into the alignment holes on the MCL/VSL layers. The PCL slid down the pins to contact the TPU, completing alignment. Manual compression temporarily held the layers together as we sandwiched the ensemble between two 25 cm × 12.5 cm large glass slides. Eleven paper binder clamps placed around the edges of the sandwich secured the layers. To ensure even pressure distribution across the device layers, we attached to the center of the sandwich a 4.5" Kant-Twist cantilever clamp (finger-tight).

For the final bonding step, we placed the sandwich in the vacuum oven at 130 ºC and -12 psi for 1.5 hrs. We visually confirmed bond completion by removing the sandwich from the vacuum oven and observing the transparency of the device layers. If hazy regions remained, we placed the sandwich back in the vacuum oven for 30 additional min. As soon as we observed near-complete transparency, we allowed the device to cool at room temperature for 40 min while remaining clamped. After cooling, we disassembled the sandwich and cut excess TPU from the edges of the device with a razor. Pressurized water, delivered for 15 min via syringe through

temporary microfluidic inlets attached to the chip surface, removed most of the PDMS base elastomer from the valve seats and the microfluidic channels. After removing the temporary inlets and drying with pressurized air, we stored the completed chip in a clean container. All 96 valves remained open throughout the bonding process and required no opening steps.

Attaching the loading frame

To create the fluid reservoir for suspending cuboids, we cut the outline of the loading frame in a sheet of 50 µm-thick adhesive (300LSE High-Strength Acrylic Pressure-Sensitive Adhesive, 3M™, USA) using a CO_2 laser system (VLS3.60, Scottsdale, USA). We attached the adhesive to the bottom face of the loading frame, then placed the frame onto the top of the MCL surface. A heat press compressed the layers at 90 psi and 60 ºC for 2 min. Last, we affixed permanent inlets by applying cyanoacrylate glue (Gorilla Super Glue, Ohio, USA) to the exterior of silicone tubes, inserting the tubes within the five inlet holes of the loading frame, filling the reservoirs around the tubes with glue, and waiting overnight.

Attaching the bottomless well plate

Following cuboid loading, we used pressure-sensitive adhesive (PSA) to adhere a bottomless well plate to the surface of the device. We found that ensuring robust adhesion between the bottomless well plate and MCL was a critical factor for effectively segregating well conditions during drug testing of cuboids. Placing the adhesive onto a wet surface would prevent bonding, while the presence of live tissue limited methods for drying the surface after the hydrodynamic capturing process. Therefore, we employed the hydrophobic protective layers of the PSA to safeguard the adhesive bonding strength from weakening by solvent exposure. First, we cut a device-sized piece of adhesive from stock using scissors. Next, we removed the protective layer from one side. Subsequently, we placed the layer adhesive-side-up onto the laser cutter to cut the stencil of the bottomless well plate. Then, during the device assembly phase, we attached the PSA to the surface of the device inside the loading frame. Thus, the second protective layer remained for the duration of the cuboid loading process, shielding the adhesive from solvent exposure. After cuboid loading, we drained solution from the loading frame reservoir via aspiration. At this point, we peeled away the second protective layer, removing trace amounts of solvent left on the hydrophobic coating. With the PSA exposed, we inserted the well plate into the loading frame and activated the adhesive by pinching the regions between each well with sterilized gloves. The PSA visibly showed bonding as cloudy regions became transparent when pressed.

Table 1: Device manufacturing parameters & dimensions

Layer	Thickness (µm)	Time to cut (mins)	Surface Profile Pts (#)	Feature	Depth (µm)	Width (µm)
microchannel layer	500	60	500	microchannels	400	700
				traps	500	800
valve seat layer	500	60	800	valve seats	50	390
				valve seat vias	500	175
pneumatic control layer	500	60	500	air channels	300	200
				actuation chambers	300	2,000
loading frame	6,350	10	32	main body	6,350	8,810
				tube inlet	6,350	3,275
bottomless well plate	6,350	30	32	interwell regions	3,700	N/A
				well wall thickness	N/A	500

Table 2: CNC milling parameters

Layer	Feature	Tool diameter (inches)	Spindle Speed (rpm)	Feed Rate (mm/min)
microchannel layer	microchannels	1/64	33k	600
	traps	1/32	28k	550
valve seat layer	valve seat	1/64 (ball mill)	33k	550
	valve seat vias	.007	28k	200
pneumatic control layer	air channels	.008	33k	260
	actuation chambers	1/32	28k	550
loading frame	main body	1/16	25k	1200
	tube inlet	1/8	12.5k	1250
well plate	wells	1/8	12.5k	1250
	interwell space	1/16	28k	2100

Supplementary Figures

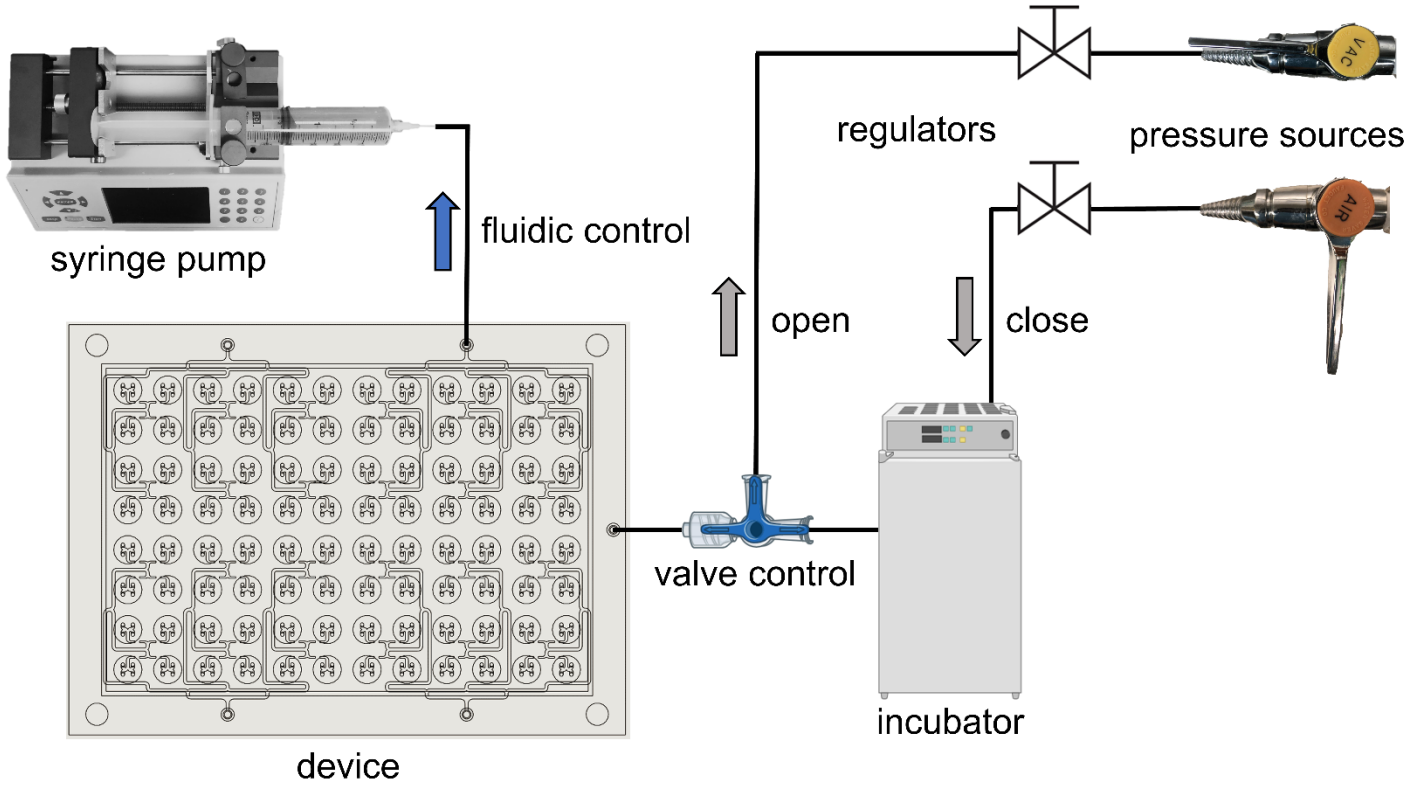

Suppl. Fig. 1. Schematic of device setup during the cuboid loading process. In a standard biosafety cabinet, pressure sources controlled by regulators connect to the valve control inlet of the device via a splitter to supply negative pressure (vacuum, for opening) or positive pressure (air, for closing). A syringe pump connects to one of four fluidic outlets to activate the cuboid traps of that respective device quadrant during cuboid loading. While loading proceeds, the pump connection transfers to other quadrants as needed. After loading, we disconnect the device from the vacuum source and the syringe pump. To enable device transfer between the biosafety cabinet and the incubator without disengaging the valves, the source of air connects to the valve control splitter via long tubing which threads through the back wall of a cell culture incubator and out the front door. For more details on the device setup before cuboid loading, see “Device preparation” in Methods.

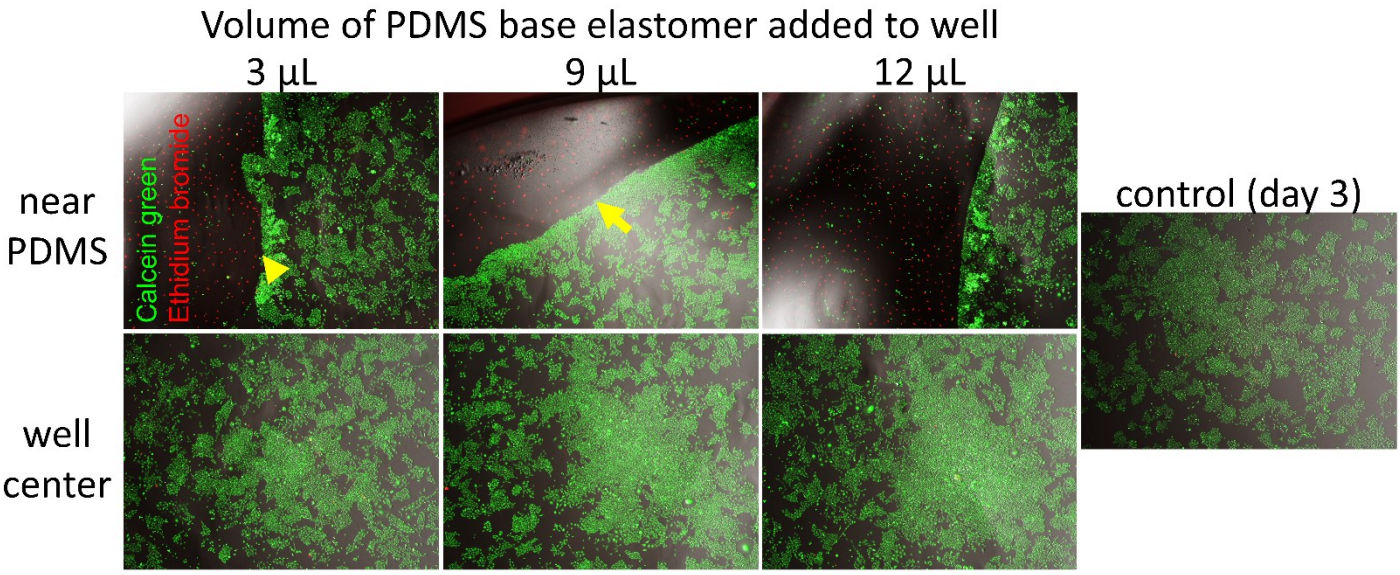

Suppl. Fig. 2. PDMS base elastomer biocompatibility analysis. To enable upscaled manufacturing of whole-thermoplastic valves, we coated the valve seats with PDMS base elastomer as an “anti-bond” solution prior to thermal fusion bonding. Washing the channels with water removed most of the elastomer, but we considered whether remaining trace amounts could affect the viability of tumor cuboids. To determine the degree of PDMS base elastomer cytotoxicity on cancer tissue, we conducted a live (calcein green) / dead (ethidium bromide) fluorescent stain analysis of Chinese hamster ovary (CHO) cells grown in a 24-well plate. We dispensed PDMS base elastomer in differing volumes within a corner of each well and observed cell viability near and far from the droplet. CHO cells continued growing in proximity to PDMS base elastomer. On day 3, proliferating cells formed a border near the PDMS droplet (yellow arrows). Cells lived (green) both on or beyond the border of the PDMS, while cells died (red) within or underneath the PDMS. Regardless of PDMS volume added to the well, cells in the well center demonstrated similar viability and morphology to the control condition, indicating no apparent culture medium toxicity from the PDMS base elastomer. (Note: glare in the images of cells near the PDMS resulted from the base elastomer reflecting light from the microscope.) From these experiments we concluded that trace quantities of PDMS base elastomer painted on the valves were not detrimental to cuboids cultured away from the valves.

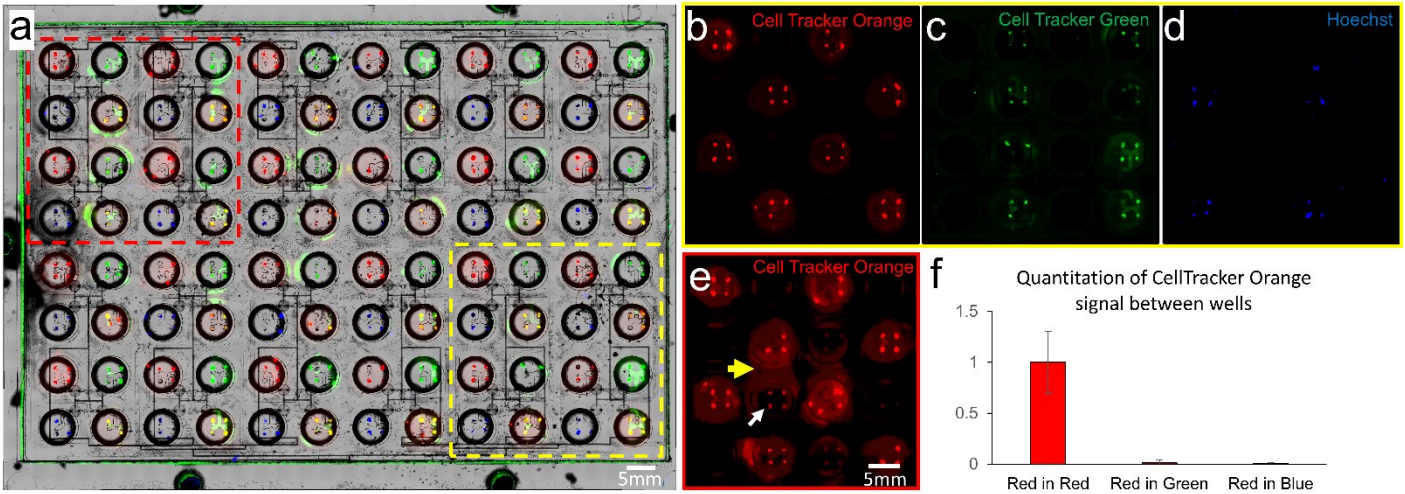

Suppl. Fig. 3. Quantification of live-cell fluorescent dye crosstalk between wells of device. (**a**) Fluorescent and brightfield overlay of device filled with live cuboids with fluidically isolated wells (closeup yellow-dashed box, **b-d** single channels) except for one region with some crosstalk through poorly bonded areas of the well plate (red-dashed box, **e**). (**b,c,d**) Representative fluorescent images of cuboids from **a** (yellow-dashed box) show prevention of fluorescent dye crosstalk between the wells for Cell Tracker Orange (CTO; b), Cell Tracker Green (CTG; c), and Hoechst (d). (**e**) Unintended staining in adjacent wells suggests low level potential crosstalk through the closed valves in the microfluidic network. However, we did not see evidence of crosstalk through the valves based on the individual fluorescence channels. In these regions, the stain had traveled beneath the walls of the wells rather than through the valves (see yellow arrow). Failure to apply enough pressure in all regions of the well plate likely contributed to bond failure in these areas. (**f**) Quantitation of CTO signal in individual cuboids demonstrates low levels in cuboids from green wells with 1.3% of the average signal seen in cuboids from red wells. The subset of 11 cuboids from green wells with poor well adherence have an average of 7%, and the remainder only have 0.2% signal. We did not quantitate Hoechst staining because of the exceptionally low signal to noise ratio. We did not quantitate green CTG staining due to background signal from the plastic and tissue autofluorescence.

Supplementary References

1. Horowitz, L. F. *et al.* Microdissected “cuboids” for microfluidic drug testing of intact tissues. *Lab Chip* **21**, 122 (2021).

2. Ogilvie, I. R. G. *et al.* Reduction of surface roughness for optical quality microfluidic devices in PMMA and COC. *Journal of Micromechanics and Microengineering* **20**, (2010).

3. Ng, S. P., Wiria, F. E. & Tay, N. B. Low Distortion Solvent Bonding of Microfluidic Chips. *Procedia Eng* **141**, 130–137 (2016).

4. Pourmand, A. *et al.* Fabrication of whole-thermoplastic normally closed microvalve, micro check valve, and micropump. *Sens Actuators B Chem* **262**, 625–636 (2018).

5. Shaegh, S. A. M. *et al.* Rapid prototyping of whole-thermoplastic microfluidics with built-in microvalves using laser ablation and thermal fusion bonding. *Sens Actuators B Chem* **255**, (2018).